

Recent Experiments in Ising Antiferromagnets with Quenched Randomness

D. P. Belanger

Physics Department, University of California
Santa Cruz, CA 95064

Received September 37, 1992

Several areas of experimentation using $d = 2$ and $d = 3$ Ising antiferromagnets with quenched randomness are reviewed. The randomly dilute $Fe_xZn_{1-x}F_2$ and $Rb_2Co_xMg_{1-x}F_4$ systems in zero field show excellent random-exchange Ising behavior for two and three dimensions, respectively. The same systems in a field are the best experimental examples of random-field Ising systems. Low-temperature domain wall dynamics have been studied in the $Fe_xZn_{1-x}F_2$ system. Spin glass-like behavior is observed in $Fe_xZn_{1-x}F_2$ near the percolation threshold, though the system is not a canonical spin glass. The canonical Ising spin glass model is realized in the $d = 3$ Ising antiferromagnet $Fe_xMn_{1-x}TiO_3$. These examples are chosen to demonstrate the opportunity of studying various Ising models with quenched randomness using insulating antiferromagnets.

I. Introduction

Insulating antiferromagnetic crystals provide a rich testing ground for theories of phase transitions. This is made possible by the universality of critical parameters characterizing phase transitions. The only properties needed to describe the asymptotic behavior upon approach to a phase transition are the basic symmetries of the system, for example the spatial dimension or the lattice geometry. Hence, theorists may study the simplest Hamiltonians having only the necessary symmetries and experimentalists need only to study simple, well understood magnetic systems with the corresponding symmetries. Insulating antiferromagnets are often ideal in this regard. The interactions between the magnetic spins decrease extremely rapidly with distance. Therefore, only a very few (often one or two) interactions characterize the behavior of many insulating magnetic crystals extraordinarily well. This simplicity has helped both theorists and experimentalists make tremendous progress on pure systems and those with quenched disorder. The subject of this review is the behavior of Ising systems with quenched disorder which can be studied in insulating antiferromagnet by growing crystals from a mixture of two isomorphous substances. For example, a mixed antiferromagnetic and diamagnetic crystal results in a system in which each possible magnetic site is randomly occupied or not. Aside from the quenched randomness, such a system may still prove quite simple in its microscopic description, with only a very few interactions needed. The rich macroscopic behavior of such simple systems is surprising and some aspects of the transitions are still not well understood.

Experiments in non-equilibrium states at low temperatures also are most readily studied in dilute magnetic systems since the interactions are very simple and easy to model. Those aspects of the problems that are now understood can be applied to much more complicated substances by virtue of universality.

The simplicity of the Hamiltonians needed to describe Ising transitions in randomly dilute antiferromagnets lends itself well to Monte Carlo simulations. Such simulations describe the observed behavior extremely well. This has led to better understanding of the theories and experiments in many cases.

We will describe some experiments, theories and simulations relating to diluted and mixed antiferromagnetic crystals. We will hopefully give a flavor of some of the interesting properties associated with quenched randomness. Some of the topics of current interest in this field will be exemplified by the examples chosen for this review. For this particular discussion, we will largely limit ourselves to the simplest, best characterized and most studied crystals. We will add comments about related systems when they add to the understanding of the models. Other systems have been discussed in previous reviews¹⁻⁸.

We begin by briefly reviewing the critical behavior of FeF_2 , which is an excellent example of a pure three-dimensional ($d = 3$) Ising model system, and K_2CoF_4 and Rb_2CoF_4 , which are excellent examples of pure $d = 2$ Ising model systems. This will help to place the experiments in the random systems into context.

We then discuss the random-exchange Ising model (REIM), which has been most accurately studied for $d = 3$ in the magnetically dilute $Fe_xZn_{1-x}F_2$ system

well above the percolation threshold $x_p = 0.24$ with no applied magnetic field. The experimental critical behavior measured in this system, both static and dynamic, will be compared with theoretical results for critical exponents and amplitude ratios. The evolution of metastable domains at low temperatures in the $Fe_xZn_{1-x}F_2$ system in zero field will be discussed as an example of the dynamics of ordering well below T_N . For $d = 2$, the best studied Ising case is $Rb_2Co_xMg_{1-x}F_4$. Again, excellent comparisons can be made between theory and experiment.

We will briefly discuss the random-field Ising model (RFIM), which can be generated by applying a magnetic field to the dilute antiferromagnet $Fe_xZn_{1-x}F_2$ system for $d = 3$ and $Rb_2Co_xMg_{1-x}F_4$ for $d = 2$. Even though many problems have been resolved, there are fundamental open questions about the $d = 3$ RFIM transition after years of intense experimental and theoretical study.

We will discuss the behavior of the three-dimensional Ising model close to the percolation threshold, primarily using the results from the Ising system $Fe_xZn_{1-x}F_2$ system. Upon approach to the percolation threshold in the Ising system, spin glass-like behavior becomes dominant. This is surprising since, although the system possesses randomness, it apparently lacks the other essential ingredient of true spin glasses, namely frustration.

A particularly clear and simple Ising spin glass system is the mixed antiferromagnet $Fe_xMn_{1-x}TiO_3$. In this insulator both frustration and randomness are present in the short-range interactions and much of the predicted spin glass behavior^{8,9} has been clearly observed.

II. The Pure Ising Model

The Ising model is one of the simplest systems exhibiting a phase transition, with each spin having only two possible states. The simplicity of the system on a microscopic scale belies the intricate and rich behavior on the macroscopic scale, especially with quenched site randomness. A simple pure Ising antiferromagnetic model Hamiltonian is

$$\mathcal{H} = \sum_{\langle i,j \rangle} JS_i S_j, \quad (1)$$

where there is only one essential interaction between neighboring spins of strength $J > 0$ and $S_i = \pm 1$. In a real system universality dictates that the asymptotic critical behavior will be described by the simple Hamiltonian above as long as the interactions are short-range. For weaker anisotropy, longer-range interactions, or multiple interactions, one must simply measure the behavior closer to the transition, i.e. the system will eventually cross over to the correct asymptotic behavior.

The pure FeF_2 system has been shown to be an excellent $d = 3$ Ising system. The critical exponent α and amplitude ratio A^+/A^- for the specific heat

$$C_p = A^\pm |t|^{-\alpha} + B \quad (2)$$

from birefringence and pulsed specific heat techniques¹⁰ agree precisely with the results of many theoretical techniques. The correlation length for fluctuations

$$\xi = \xi_0^\pm |t|^{-\nu} \quad (3)$$

and the staggered susceptibility

$$\chi_s = \chi_0^\pm |t|^{-\gamma}, \quad (4)$$

have been obtained from neutron scattering experiments¹¹, the staggered magnetization

$$M_s = M_0 |t|^\beta, \quad (5)$$

which is only nonzero for $t < 0$, from Mössbauer experiments¹², and the dynamic critical behavior for the relaxation times

$$\tau \sim \xi^z. \quad (6)$$

from spin-echo neutron scattering techniques¹³. All of the critical behavior measured over the critical range $|t| < 0.02$ in pure FeF_2 is in superb agreement with theory¹⁴⁻¹⁸. The observation of asymptotic behavior over such a large range of $|t|$ is a result of the strong single-ion anisotropy and the simplicity of the magnetic interactions in pure FeF_2 . The magnetic ions form a tetragonal body-centered lattice and the exchange interaction between the body center and corner ions is the only significant one¹⁹.

The critical parameters measured for the pure Ising model using the FeF_2 system are summarized in Table I along with relevant theoretical results. It is important to realize that the universal ratios of the amplitudes are just as important in characterizing the critical behavior as the exponents. The results demonstrate that FeF_2 is an exemplary Ising system and, upon dilution, an ideal one to study the effects of random-exchange and random-fields for $d = 3$.

The pure $d = 2$ Ising transition is very well represented by the isomorphic antiferromagnets K_2CoF_4 and Rb_2CoF_4 . The interactions between the planes of magnetic Co^{2+} ions are extremely small compared to the interactions within the planes. The specific heat behavior has been measured²⁰ using birefringence techniques in Rb_2CoF_4 . From the Onsager solution²¹ of the $d = 2$ Ising model, we expect the specific heat to be consistent with the asymptotic logarithmic form

$$C_p = A \ln(|t|) + B. \quad (7)$$

The data indeed agree well with this form. The critical behavior of ξ , χ_s and M_s have been obtained using

neutron scattering techniques²². The static critical behavior exponents and amplitude ratios are consistent with theory^{21,23}. In addition, the two-scale universal ratio²⁴

$$R_s = \chi_0^+ \kappa_0^{+d} / M_0, \quad (8)$$

has been demonstrated^{22,25} in these compounds. The results of experiments on these systems and comparisons to theory are summarized in Table I. These systems, when diluted, are obvious choices for investigating random-exchange and random-field effects in two dimensions.

Table I: Experimental and Theoretical Pure Ising Critical Parameters. The definitions for the exponents and amplitudes can be found in Eq. (2-8). All $d = 3$ experimental parameters are obtained from FeF_2 . The parameters for $d = 2$ were obtained using Rb_2CoF_4 or K_2CoF_4 . Superscripts + or - refer to those obtained for ν and γ using only data for $1 > 0$ and $1 < 0$, respectively.

$d = 2$ PURE ISING

	Experiment	Theory
α	0.00 ± 0.01^a	$0(\log t)^b$
A^+/A^-	1.01 ± 0.00^a	$1(\log t)^b$
ν	$1.02 \pm 0.05^{+c}$ 1.12 ± 1.13^{-c}	1^b
κ_0^+/κ_0^-	0.54 ± 0.06^c	$1/2^d$
γ	$1.82 \pm 0.07^{+c}$ 1.92 ± 0.20^{-c}	$7/4^e$
χ_0^+/χ_0^-	32.6 ± 3.7^c	37.33^d
β	0.155 ± 0.02^c	$1/8^b$
R_s	$0.0565^c, 0.043^e$	0.051^f

$d = 3$ PURE ISING

	Experiment	Theory
α	0.11 ± 0.005^g	0.11 ± 0.003^h
A^+/A^-	0.54 ± 0.025^i	0.55^h
ν	0.64 ± 0.01^j	0.630 ± 0.001
κ_0^+/κ_0^-	0.53 ± 0.01^j	0.52^i
γ	1.25 ± 0.02^j	1.240 ± 0.001^h
χ_0^+/χ_0^-	4.6 ± 0.2^j	4.8^i
β	0.325 ± 0.005^m	0.325 ± 0.001^h
Z	2.1 ± 0.1^l	1.05 ± 0.07^m

a)ref.[20]; b)ref.[21]; c)ref.[22]; d)ref.[23,17]; e)ref.[25]; f)ref.[24]; g)ref.[10]; h)ref.[14]; i)ref.[15]; j)ref.[11]; k)ref.[12]; l)ref.[13]; m)ref.[18].

An important point should be made concerning the measurement of the staggered magnetization with neutron scattering techniques. In the $d = 3$ case, the samples are typically of such high crystalline quality that those neutrons aligned well enough to Bragg scatter do so in the first few microns of the crystal. This results in

a saturation effect in the observed scattering intensity, an effect known as extinction. Recently, neutron Bragg scattering in epitaxial thin films has been successful in showing the proper behavior²⁶ of the staggered magnetization in pure and dilute Ising antiferromagnets. For the case of $d = 2$ magnetic systems, extinction is not a problem because the order parameter scattering takes place along one-dimensional rods in reciprocal space and not at points as is the case for $d = 3$. As a result, the scattering is not saturated in bulk samples and the proper critical behavior is observed.

111. The Random-Exchange Ising Model

A simple random-exchange Ising model Hamiltonian for a single interaction site-diluted antiferromagnet is

$$\mathcal{H} = \sum_{\langle i,j \rangle} J_{ij} \epsilon_i \epsilon_j S_i S_j, \quad (9)$$

where ϵ_i is unity if the site is occupied and zero otherwise. No external field is applied in this model and there are no frustrated interactions. This model can be realized to high accuracy for $d = 3$ in the $Fe_x Zn_{1-x} F_2$ antiferromagnet²⁷. Similarly, the corresponding two-dimensional REIM is extremely well represented by the magnetically dilute antiferromagnet $Rb_2 Co_x Mg_{1-x} F_4$.

The most basic effect of dilution on an unfrustrated Ising system is the lowering of the transition temperature $T_N(x)$. There is a limit, the percolation threshold at concentration x_p , below which no transition can take place since the magnetic spins cannot form a long-range network. For concentrations well above x_p , it is found from both CPA theory²⁸ and experiments²⁹ in the $d = 3$ Ising system $Fe_x Zn_{1-x} F_2$ that $T_N(x)/T_N(1) \approx x$. For the $d = 2$ system $Rb_2 Co_x Mg_{1-x} F_4$ an approximately linear decrease is observed above the percolation threshold³⁰. The transition temperature inevitably drops precipitously near the percolation threshold for both $d = 2$ and $d = 3$.

The specific heat critical behavior in a $d = 3$ REIM system is fundamentally different from the pure case. As first pointed out by Harris³¹, the specific heat cannot be positive for a system with quenched dilution if the hyperscaling relation $2 - \nu d = \alpha$ holds, as it does in the REIM. (It does not hold for the RFIM.) In the $d = 3$ Ising case this implies a crossover from the pure transition for which $\alpha > 0$. The greater the dilution, the larger the region of reduced temperature over which the REIM behavior is observed. Contrary to early theoretical expectations³², the crossover occurs quite rapidly^{33,34}. The new, REIM specific heat critical behavior has been measured³⁵ for $Fe_{0.6} Zn_{0.4} F_2$ and more recently³⁶ for $Fe_{0.85} Zn_{0.15} F_2$, using the optical birefringence technique³⁷. The latter case is shown in Fig. 1. The most recent preliminary result $\alpha = -0.9 \pm 0.02$, using Eq. 2 agrees very well with theory^{38,39} and the

previous experiment. The most recent amplitude ratio, $A^+/A^- = 1.55 \pm 0.15$ agrees well with the previous result but does not agree with theories^{40,41} which yield $A^+/A^- < 0$. The predicted behavior is unusual. The specific heat would appear as an inflection rather than a cusp. The experimental results are completely incompatible with such behavior for reduced temperatures as small as $|t| = 10^{-4}$. This most likely reflects an inadequacy of the theory and remains an outstanding theoretical problem.

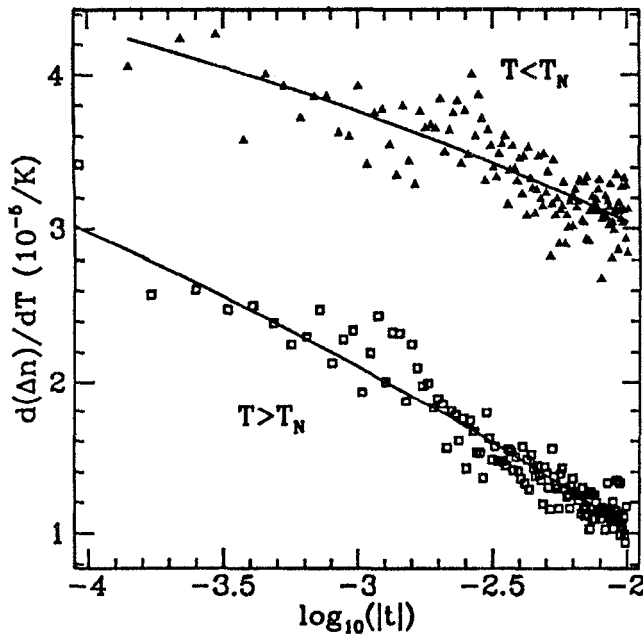


Figure 1: The temperature derivative of the optical birefringence $d(\Delta n)/dT$, which is proportional to the magnetic specific heat³⁷, vs. T for the $d = 3$ Ising antiferromagnet $Fe_{0.85}Zn_{0.15}F_2$. The solid curves indicate a fit to several sets of data using the power law behavior in Eq. 2 yielding the parameters given in Table II. The data indicate a cusp and not the inflection suggested by theory⁴¹. (Wang and Belanger³⁶).

Quasielastic neutron scattering studies⁴² of $Fe_{0.46}Zn_{0.54}F_2$ have yielded the critical parameters for ξ , and χ using Lorentzian line shapes, which work well despite predictions for non-Lorentzian contributions⁴³. Mossbauer experiments^{33,44} have been used to determine the exponent for M . Spin-echo neutron scattering techniques¹³ have shown that the critical dynamics of $Fe_{0.46}Zn_{0.54}F_2$ are well approximated by conventional theory¹⁸, but with relaxation times two orders of magnitude longer than for pure FeF_2 . All of the measured critical parameters and their calculated values⁴⁵⁻⁴⁷ for the $d = 3$ REIM are listed in Table II.

The $d = 2$ specific heat, best exemplified by measurements using the optical birefringence technique⁴⁸ in the $Rb_2Co_{0.85}Mg_{0.15}F_2$ system, is a marginal case with respect to the Harris criterion, since in the pure system α is zero (logarithmic divergence). Theories^{45,46} for the

random-exchange behavior predict the asymptotic behavior

$$C_p \sim \log(\log(|t|)) \quad (10)$$

The experimental data are well described by a logarithmic divergence, as shown in Fig. 2. It would be incredibly difficult in experiments to distinguish between fits of the data to the double logarithm in Eq. 10 and fits to the single logarithm of Eq. 7. Hence, the experiments are consistent with the theories, though perhaps not a definitive test of them. In the two-dimensional system $Rb_2Co_xMg_{1-x}F_4$, neutron scattering measurements⁴⁹ provide the critical behavior of ξ , χ and M . In addition, a two-scale universality analysis yields a value close to that obtained in the pure material. The experimental and theoretical results are summarized in Table II.

Table II: Experimental and Theoretical Random-Exchange Ising Critical Parameters. The definitions for the exponents and amplitudes can be found in Eq. (2-8). All $d = 3$ experimental parameters are obtained from $Fe_xZn_{1-x}F_2$. The parameters for $d = 2$ were obtained using $Rb_2Co_xMg_{1-x}F_4$. Superscripts $+$ or $-$ refer to those obtained for ν and γ using only data for $t > 0$ and $t < 0$, respectively.

$d = 2$ RANDOM-EXCHANGE ISING

	Experiment	Theory
α	$\approx O(\log t)^a$	$O(\log(\log t))^b$
A^+/A^-	0.05 ± 0.10^m	$1(\log(\log t))^b$
ν	$1.08 \pm 0.06^{+c}$	$1^d, 1002^e$
	1.58 ± 0.52^{-c}	
κ_0^+/κ_0^-	0.98 ± 0.02^l	
γ	$1.75 \pm 0.07^{+c}$	1.753^e
	2.6 ± 0.6^{-c}	
χ_0^+/χ_0^-	19.1 ± 5.0^c	-
β	0.13 ± 0.02^l	-
R_s	0.062 ± 0.01^l	-

$d = 3$ RANDOM-EXCHANGE ISING

	Experiment	Theory
α	-0.09 ± 0.02^f	$-0.099, -0.03^h - 0.01^e$
A^+/A^-	1.55 ± 0.15^f	-0.5^i
ν	0.69 ± 0.01^j	$0.70^g, 0.68^h, 0.67^e$
κ_0^+/κ_0^-	0.69 ± 0.02^j	0.83^i
γ	1.31 ± 0.03^j	$1.39^g, 1.34^h, 1.32^e$
χ_0^+/χ_0^-	2.8 ± 0.2^j	1.7^i
β	0.35 ± 0.01^k	$0.349 \pm 0.002^h, 0.348^e$
Z	1.7 ± 0.2^l	2.3^m

a)ref.[48]; b)ref.[45,46]; c)ref.[49]; d) pure value; e)ref.[47]; f)ref.[36]; g)ref.[38]; h)ref.[39]; i)ref.[40]; j)ref.[42]; k)ref.[33,44]; l)ref.[13]; m)ref.[18].

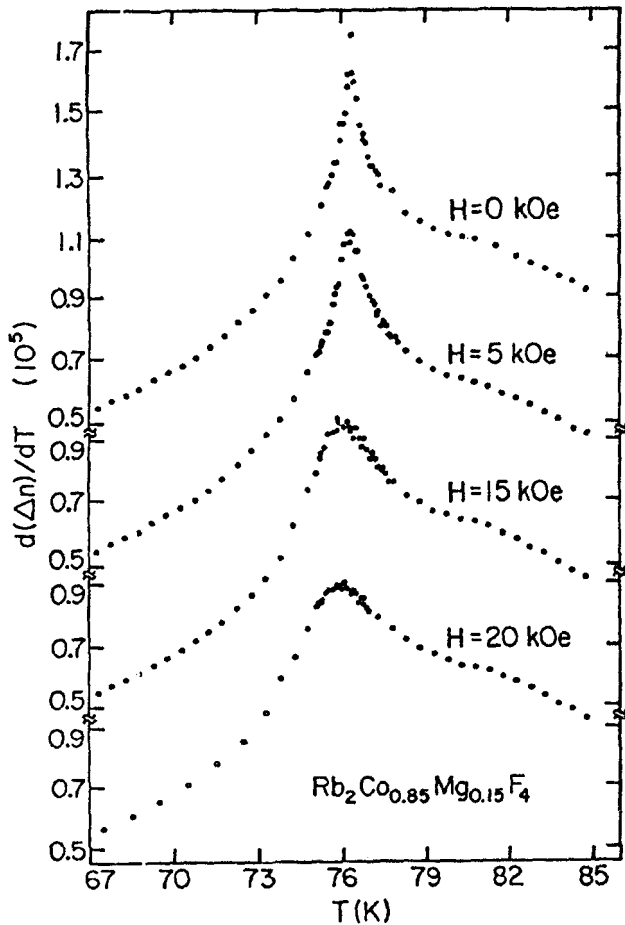


Figure 2: $d(\Delta n)/dT$ vs. T for the $d = 2$ Ising antiferromagnet $Rb_2Co_{0.85}Mg_{0.15}F_4$ in applied fields $H = 0, 0.5, 1.5,$ and $2.0T$. The data sets are offset for clarity. The $H = 0$ peak is approximated by a symmetric logarithmic divergence. The rounding of the peak increases with H and occurs in equilibrium, indicating that the transition is destroyed by the random-field. (Ferreira, et al.[48]).

IV. The Random-Field Ising Model

A random-field Ising ferromagnet may be represented most simply by a Hamiltonian such as

$$\mathcal{H} = - \sum_{\langle i,j \rangle} J S_i S_j - \sum_i h_i S_i, \quad (11)$$

where the field satisfies the conditions $[h_i]_{av} = 0$ and $[h_i^2]_{av} = h_r^2$, with $[]_{av}$ signifying an average over the quenched disorder. It is quite difficult to realize such a Hamiltonian directly in a real magnet with a controllable random-field strength. Instead, the RFIM is studied in dilute Ising antiferromagnets with a uniform field applied in the spin ordering direction. A simple Hamiltonian corresponding to an antiferromagnet with random field is

$$\mathcal{H} = \sum_{\langle i,j \rangle} J_{ij} \epsilon_i \epsilon_j S_i S_j - \sum_i H \epsilon_i S_i, \quad (12)$$

where H is a uniform field. The analogy of the two systems was first pointed out by Fishman and Aharony³². In the original random-field ferromagnetic model⁵⁰, the local fluctuations in the net random field compete with the long-range ferromagnetic order. In the dilute antiferromagnet, the local fluctuations in the sublattice populations tends locally to favor one sublattice over the other to point along the uniform field, in direct competition with the antiferromagnetic long-range order. This analogy was taken further by Cardy⁵¹, who showed that the static critical behavior of a ferromagnet in a random field is identical to that of a dilute antiferromagnet in a uniform field. The random and uniform fields are related by

$$h_r^2 = \frac{x(1-x)[T^{MF}/T]^2 (g\mu_B S H / k_B T)^2}{[1 + \Theta^{MF}(x)/T]^2}, \quad (13)$$

where x is the concentration, T^{MF} is the pure system mean-field transition temperature and Θ^{MF} the Curie-Weiss susceptibility parameter.

The early investigations of the RFIM were marked by a controversy over whether a phase transition actually took place for $d = 3$. This was a particularly difficult theoretical question to answer, though some of the first experiments⁵², using the birefringence technique to measure the specific heat critical behavior, yielded strong evidence for a transition. In contrast to these conclusions, poor sample quality and a poor appreciation for the strong hysteresis in the dilute antiferromagnets did result in some groups claiming that the transition was destroyed. The rigorous theories of Imbrie⁵³ and Bricmont and Kupiainen⁵⁴ proved the validity of the conclusions of the early birefringence measurements.

Efforts now are being made to fully calculate⁵⁵ and measure the $d = 3$ RFIM critical behavior. From neutron scattering measurements⁵⁶, the correlation length appears to diverge with an exponent $\nu \approx 1$, and the exponent for ξ is approximately $\gamma = 1.75$. The specific heat appears to be close to a symmetric, logarithmic divergence⁵². Curiously, these values are all close to those of the pure $d = 2$ Ising model. Early theoretical works in fact predicted an effective dimensional reduction in the critical behavior⁵⁷⁻⁵⁹. However, it was supposed to be from three to one dimension. Since there is no transition in the $d = 1$ Ising model, the implication was that there would be no transition for the $d = 3$ RFIM, a result later shown to be incorrect. Dimensional reduction is no longer generally supported by theorists.

The one exponent which is still only roughly determined⁶⁰ is the staggered magnetization exponent,

β . This is primarily a result of the severe extinction of the neutron scattering intensity encountered in the $d = 3$ crystals. The measurement of this exponent is of crucial importance for testing the RFIAI critical behavior theories.

The crossover from the random-exchange to the random-field Ising behavior depends upon the strength of the random-field which in turn varies linearly with the strength of the applied field³⁴. The random-field scaling behavior dictates that the transition boundary in the $H - T$ phase diagram varies as

$$T_c(H) - T_N \approx H^{2/\phi} \quad (14)$$

where the crossover exponent $4 \approx 1.1\gamma$ with γ being the random-exchange staggered susceptibility exponent⁶¹. This behavior has been verified⁶² by experiments on $Fe_xZn_{1-x}F_2$, with the results $\gamma = 1.31 \pm 0.03$ and the value from many measurements⁶³ $\phi = 1.42 \pm 0.03$. Some of the earlier experiments leading to the conclusion that the pure value of γ were adversely affected by concentration gradients and the practice of taking the transition to be at the peak in the specific heat, as shown by simulations⁶⁴.

The dynamics of the $d = 3$ RFIAI have now been convincingly demonstrated, using ac susceptibility measurements^{65,66}, to be activated in $Fe_xZn_{1-x}F_2$ in agreement with theory^{67,68}. Spin-echo neutron scattering measurements show¹³ that, on the very short time scale of nanoseconds, the system crosses over to random-field dynamics at much larger reduced temperatures and much lower applied fields than measurements which are conducted on time scales of seconds, such as specific heat or quasielastic neutron scattering. Extremely slow dynamics are manifest in two distinct ways near the transition. First, when cooling in a field (FC) or heating in a field after cooling in zero field (ZFC), equilibrium is lost near the transition. Upon FC, the system cannot achieve long-range order and the data differ from the ZFC data below an equilibrium boundary $T_{eq}(H)$ which lies just above $T_c(H)$ and scales in precisely the same manner. Of course, with a small enough random field and limited instrumental resolution, the FC procedure will appear to yield long-range order⁶⁹.

Closer to $T_c(H)$, the critical behavior is rounded by the critical slowing, as exemplified by the ZFC Faraday rotation data⁷ in Fig. 3. Shapiro^{71,5} has proposed a theory based on the slow dynamics which predicts the observed critical exponents.

The neutron scattering line shapes observed in the $d = 3$ RFIM systems are far from the Lorentzian form which adequately describes the scattering in pure FeF_2 and in $Fe_xZn_{1-x}F_2$ in zero field well above the percolation threshold. Mean-field theory predicts a squared Lorentzian line shape and it has been commonly assumed that the mean-field argument adequately explains the unusual observed line shapes. However, al-

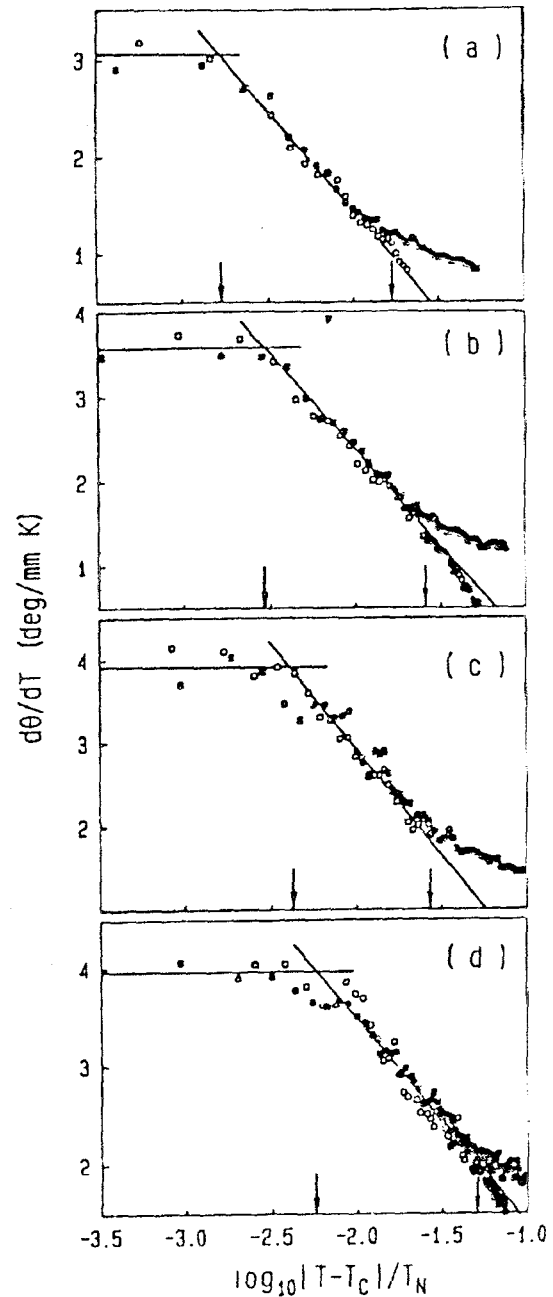


Figure 3: $d\theta/dT$, which is proportional to the magnetic specific heat⁷⁸, vs. $\log_{10}(|t|)$ upon FC in the $d = 3$ Ising antiferromagnet $Fe_{0.47}Zn_{0.53}F_2$ for $H = 2, 3, 4$ and $5T$ in (a), (b), (c), and (d), respectively. In each figure the filled symbols are for $T < T_c(H)$ and the open ones for $T > T_c(H)$. The right arrow indicates where the random-exchange to random-field crossover occurs. The left arrow in each case indicates the onset of rounding from RF dynamics. Both the region of RF dynamics and the region of RFIM critical behavior increase in size with increasing field. Data between the arrows in each case are seen to approximate a symmetric, logarithmic divergence. (Pollak, et. al.[70]).

though the squared Lorentzian works well for low temperature FC scans and scans above T_{eq} it does not work well⁶² for ZFC scans below $T_c(H)$. Furthermore, non-Lorentzian line shapes are observed⁷² at zero field in the nonequilibrium region near the percolation threshold but not observed⁷³ in the $d = 2$ case for $H > 0$ near T_N where the destruction of the transition occurs in equilibrium. All of these observations suggest a nonequilibrium origin to the non-Lorentzian line shapes near $T_c(H)$ for $d = 3$.

For the $d = 2$ RFIM system $Rb_2Co_{0.85}Mg_{0.15}F_4$, the transition is observed to be destroyed⁴⁸, as shown in Fig. 2, in agreement with theory⁵⁰. No hysteresis or extremely slow dynamics are observed near the destroyed transition, indicating equilibrium behavior. At low temperatures, however, metastable long-range order induced by ZFC decays only when the rounded transition is approached sufficiently closely. This occurs closer to the transition as the measurement time scale decreases, as indicated by the comparison of high field pulsed magnetization experiments⁷⁴ and neutron scattering measurements⁷⁵ which differ in the measurement time scale by eight orders of magnitude.

V. Metastable Domain Wall Dynamics

Random-exchange interactions not only affect the phase transition to long-range order in a profound way, but also the equilibrium dynamics for $T \ll T_N$. The fact that the interactions in $Fe_xZn_{1-x}F_2$ are so well understood and are very simple makes this system ideal for investigating the dynamics of metastable domain walls at low temperature. Domain walls may be conveniently introduced into the system by FC. The length scale associated with the domains, as evident from the widths of neutron scattering line profiles⁷⁶, decreases as the strength of the applied field upon FC increases. Two distinct kinds of dynamics can be investigated. With a field applied the evolution of the domains will be influenced by pinning from the random field as well as from vacancies. Once the field is removed, on the other hand, the only pinning remaining is from the vacancies. We shall discuss the latter case first.

At low enough temperatures, it has been shown from neutron scattering⁷⁷ and Faraday rotation experiments^{78,70} that the domain walls do not move macroscopically even after the field is removed. A common misconception is that the width of the neutron scattering profiles yields directly the size of metastable domains. Computer simulations⁷⁹ demonstrate, however, that the magnetic system forms essentially only two domains that are incredibly intertwined, as shown in Fig. 4. At best, the non-Lorentzian width represents the typical distance needed to pass from one domain to the other. Nowak and Usadel⁸⁰ suggest that the domains are fractal in structure. The line shape has been studied with Monte Carlo simulations⁸¹ and has

some unusual properties associated with the fractal-like structure.

The fact that the domain structure does not evolve on a macroscopic scale at low temperatures indicates that the thermal fluctuations are not strong enough to overcome the vacancy pinning. The walls evolve on a microscopic scale, however. Early experiments⁷⁰ showed a time dependence to the remanent magnetization after the field is turned off at low temperatures. The remanent magnetization originates from the domain walls formed upon FC. The domain walls have magnetization since, upon cooling in a field, the spins on either side of the domain wall are parallel to the field to reduce the local random-field free energy. Once the field is removed, there is no energetic advantage to alignment with the field. The domain walls then evolve in such a way as to locally minimize the exchange energy, i.e. the surface area of the walls is reduced. Spins along the wall which were predominantly aligned with the field will flip as the wall translates by one lattice spacing. This provides the mechanism by which microscopic wall movements, driven by the exchange energy, reduce the net magnetization⁸².

Nattermann and Villain^{6,83} initiated the idea that microscopic wall movements and not macroscopic motion constituted the mechanism for the decay of the remanent magnetization and attempt to explain the original experimental results. They proposed the decay

$$M_s = M_0 \ln(|t|)^{-\psi} + B, \quad (15)$$

where $\psi \approx 0.4$ and B is a constant volume term which is small, to describe the experimental results⁷⁰ for $Fe_{0.47}Zn_{0.53}F_2$. Later Monte Carlo simulation data obtained by Nowak and Usadel⁸⁰ using a simple-cubic lattice showed better agreement with the power law behavior

$$M_s \sim |t|^{-x} \quad (16)$$

and attributed the behavior to a lack of a characteristic length scale associated with the fractal domains.

Further experimental studies⁸⁵ and Monte Carlo simulations⁸² indicate another expression which does an excellent job of describing the data for the body-centered tetragonal lattice of dilute $Fe_{0.47}Zn_{0.53}F_2$ and a simulated body-centered cubic lattice. The expression,

$$M_s = M_0 \exp[(-A \ln |t|)^\psi], \quad (17)$$

yields exceptionally good fits of the data with ψ independent of the field and temperature. A suitable theory for this form is lacking.

The dynamics associated with domain wall pinning by random fields have been studied⁸⁴ by employing the FC procedure at temperatures not far below $T_c(H)$ and measuring the time dependence of the uniform magnetization in the presence of the field using SQUID techniques. Apparently, at such temperatures the random-field pinning dominates over the vacancy pinning and

many of the observations are consistent with the theoretical models for low-temperature random-field activated dynamics⁸⁷. This implies that there must be many small activated domains as opposed to the fractal-like, two-domain, frozen structure existing at low temperature.

VI. The Percolation Threshold in the Ising Model

The $d = 3$ Ising model system $Fe_xZn_{1-x}F_2$ near the percolation threshold provided some experimental surprises. Earlier experiments⁸⁸ on the weakly anisotropic, isomorphic antiferromagnet $Mn_xZn_{1-x}F_2$ were interpreted in terms of a geometric correlation length, κ_G , and a thermal correlation length. For all concentrations above the percolation threshold in the weakly anisotropic system, long-range order was observed and equilibrium behavior seemed to prevail for all temperatures. Such is not the case for the Ising system. In zero field, even a few percent above the percolation threshold, long-range order does not develop. Instead, near the percolation threshold a spin glass-like phase is encountered^{7,89,90}. Yet this system cannot be considered a canonical spin glass which requires two ingredients, randomness and frustration. In zero field, there is little or no frustration¹⁹ in $Fe_xZn_{1-x}F_2$. Nevertheless, in the $H - T$ phase diagram there is a boundary which is completely analogous to the spin glass de Almeida-Thouless (AT) boundary⁹¹ including the scaling exponent $\phi \approx 3.4$. This was first observed in magnetization studies by Montenegro, et al.^{89,90}. Even in zero field no long-range order develops⁷² for $x \leq 0.27$ and unusual line shapes are evident for $T < 12K$. A bit further above the percolation threshold, at $x = 0.31$, both the usual random-field behavior at low H and the spin glass-like behavior at higher H exist^{90,92}, as shown in the $H - T$ phase diagram in Fig. 5. The random-field behavior at low H is the same as that seen for all H at higher concentrations $x \geq 0.46$. At higher fields, the equilibrium boundary scaling with $\phi \approx 3.4$ appears. No long-range order persists in the region at high field. It has been shown⁷⁹ in Monte Carlo simulations, in which it is assured that there are no frustrating interactions, that a phase diagram very much like that seen in $Fe_xZn_{1-x}F_2$ emerges. It is interesting to note that the observation of such behavior may be indicative of quenched randomness rather than simply a manifestation of a spin glass system, as is commonly assumed. The underlying physics causing the spin glass-like behavior in $Fe_xZn_{1-x}F_2$ must be related to the extremely slow dynamics associated with the Ising percolation threshold⁹³. A complete understanding of the behavior in this system is important in itself and may shed light on the spin glass problem as well.

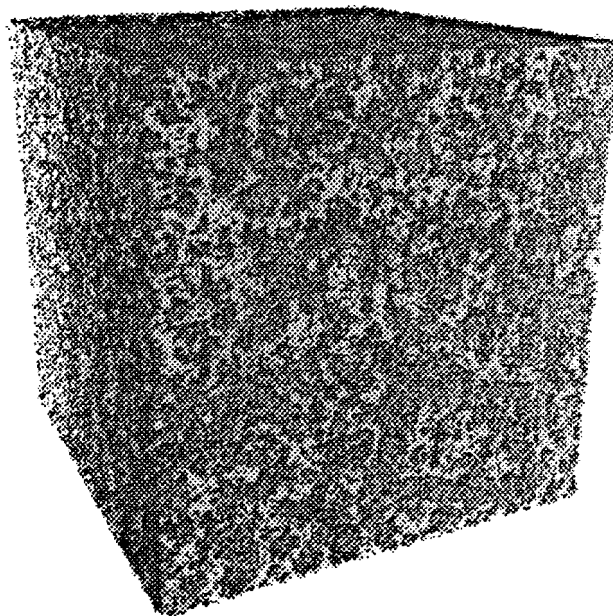


Figure 4: A computer simulation of a dilute ($x = 0.5$) antiferromagnet cooled in a magnetic field to low temperature. The lattice size is $99 \times 99 \times 98$ and it was FC with $H = 3J$. The light and dark shades represent spins belonging to the two connected domains which interweave in a fractal-like structure. (Nowak and Usadel [79]).

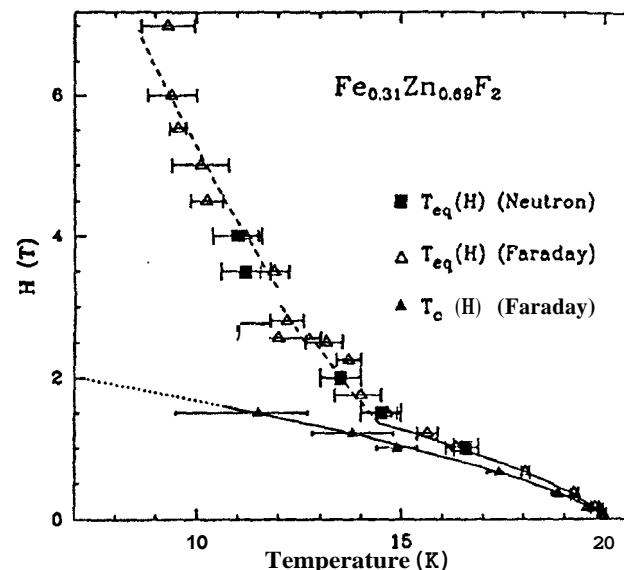


Figure 5: H vs. T phase diagram for $Fe_{0.31}Zn_{0.69}F_2$. For $H < 1.5T$, $T_{eq}(H)$ and $T_c(H)$ scale with $\phi = 1.4$, the RFIM crossover exponent. For $H > 2T$, $T_{eq}(H)$ changes curvature and scales with $\phi = 3.4$. The region below $T_c(H)$ exhibits antiferromagnetic long-range order. The region below $T_{eq}(H)$ and above $T_c(H)$ is not antiferromagnetic. (Montenegro, et al. [92]).

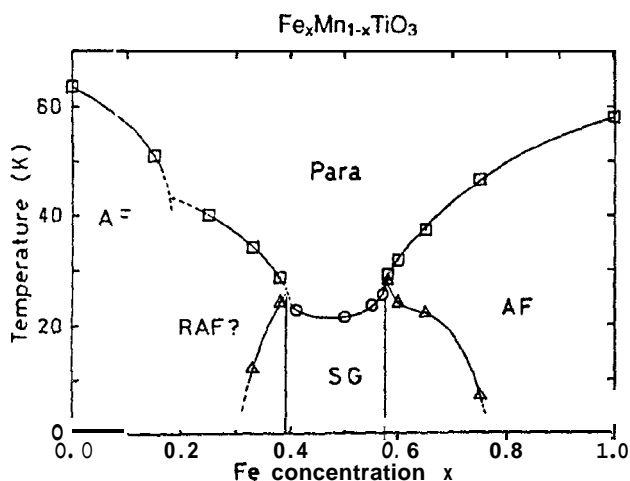


Figure 6: The $x - T$ phase diagram for the spin glass system $Fe_xMn_{1-x}TiO_3$. For concentrations $0.4 < x < 0.6$, a spin glass phase is encountered as T is lowered. Just to either side of this region, upon lowering T , a transition from paramagnetism to antiferromagnetism occurs and, at lower T , a mixed antiferromagnetic/spin glass region is entered. (Yoshizawa, et al.[96]).

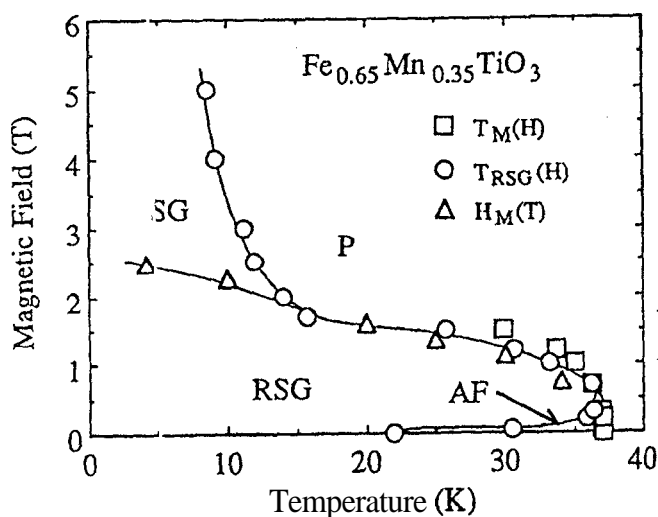


Figure 7: The $H - T$ phase diagram for the spin glass system $Fe_{0.65}Mn_{0.35}TiO_3$. At $H = 0$, the system undergoes a transition to antiferromagnetic long-range order and then, at lower T enters the mixed region. At high H , a spin glass region separates the mixed region from the paramagnetic region. There are significant similarities and differences between this spin glass phase diagram and the one for near the Ising percolation threshold shown in Fig. 5. (Yoshizawa, et al.[96]).

VII. Ising Spin Glass in Mixed Antiferromagnets

Finally, we discuss an example of an Ising spin glass system, $Fe_xMn_{1-x}TiO_3$, formed by the random mixing of two Ising antiferromagnets⁹⁴⁻⁹⁶. The pure systems $FeTiO_3$ and $MnTiO_3$ are both Ising antiferromagnets with spin alignments along the same crystalline axis but with very different spin arrangements in the ordered state. In the mixed system, each spin encounters a random environment of ferromagnetic and antiferromagnetic interactions with its neighbors. Hence, interactions in the mixed system possess both randomness and frustration, the two essential ingredients for a canonical spin glass. This is perhaps the finest example of an insulating antiferromagnetic Ising spin glass.

Mean-field theories for spin glasses yield a phase diagram in which the spin glass transition is encountered as the temperature decreases in the presence of a large amount of randomness. For the case of less randomness, the sample undergoes a transition to antiferromagnetic long-range order and then, at lower temperature, a mixed region is entered as the AT boundary is crossed. The mixed region corresponds to both long-range order and a spin glass order. Between the mixed region and the spin glass region is a vertical boundary. In the $Fe_xMn_{1-x}TiO_3$ system⁹⁴, the spin glass region occurs for concentrations between $x \approx 0.4$ and 0.6 as shown in the $x - T$ phase diagram in Fig. 6. This is the region of greatest randomness. Antiferromagnetic regions, with mixed regions at lower temperatures, exist to either side of the spin glass region, consistent with the mean-field diagram.

Elastic scattering measurements at the antiferromagnetic scattering point in sample at a concentration $x = 0.60$ in the antiferromagnetic/mixed region show an abrupt increase in intensity at the Bragg point upon lowering the temperature through the antiferromagnetic transition, as would be expected for a transition to antiferromagnetic long-range order. Then, upon crossing the AT line, the intensity sharply decreases. In the mixed region, the width of the Bragg scattering peak remains resolution limited and no sign of hysteresis is observed. This indicates that the observed behavior is the equilibrium behavior and, therefore, the long-range antiferromagnetic order decreases upon entering the mixed region. Concomitantly, the short-range antiferromagnetic order increases as the mixed phase is entered. The correlation length for antiferromagnetic fluctuations appears to diverge at the antiferromagnetic transition and shows another maximum at the crossing of the AT line. At low temperatures, the diffuse scattering profiles have a width reflecting a geometric disorder which appears to vanish at the boundary between the mixed and spin glass phases. Sharp excitations are supported⁹⁵ by the system only for $q < \kappa_G$.

The $H - T$ phase diagrams of this material for

$x = 0.6, 0.65$ and 0.75 have been measured⁹⁶. An example is shown in Fig. 7. At low fields an antiferromagnetic region exists but a spin glass region dominates at higher field. Some aspects of this phase diagram resemble that of $Fe_{0.31}Zn_{0.69}F_2$ shown in Fig. 5. There is a transition from paramagnetism to antiferromagnetism at low fields and at high fields there is an AT-like boundary between the paramagnetic and spin glass regions. However there are significant differences. No clear reentrance region is defined in the $Fe_{0.31}Zn_{0.69}F_2$ system as there is in $Fe_{0.65}Mn_{0.35}TiO_3$. The Bragg scattering shows no hysteresis in $Fe_{0.65}Mn_{0.35}TiO_3$, whereas it is evident in $Fe_{0.31}Zn_{0.69}F_2$. Lorentzian line shapes are adequate for $Fe_{0.65}Mn_{0.35}TiO_3$ for $H = 0$, but not for $Fe_{0.31}Zn_{0.69}F_2$ at low temperatures. The differences and similarities are interesting and need to be understood for a complete understanding of both the spin glass and Ising percolation threshold models.

VIII. Concluding Remarks

We have seen several examples of models of randomness realized by simple insulating antiferromagnets. The experiments done on these and other antiferromagnets with quenched randomness have helped tremendously in the understanding of the general role randomness plays in phase transitions and the behavior of ordered systems. The simple nature of the interactions has allowed theoretical treatments and computer simulations to elucidate the observed behavior. Experiments on $d = 3$ REIM systems confirmed the prediction of a crossover to a new universality class. Only minor problems still need to be solved to bring REIM experiments and theory into complete agreement. Strong evidence for the $d = 3$ RFIM transition was observed in some experiments long before theorists finally proved its existence. Theories, simulations and experiments are now directed at understanding the phase transition in detail. Near the percolation threshold the observation of spin glass-like behavior in Ising antiferromagnets has been corroborated by computer simulations and is indicated by some theory, but a complete understanding is still lacking. A better understanding of the common appearance of an AT line in canonical Ising spin glasses and in dilute Ising antiferromagnets near the percolation threshold is needed. The decay of the remanent magnetization in dilute Ising antiferromagnets for $T < T_N$ may lead to a better understanding of nonequilibrium processes if proper theories can be developed to explain the observed behavior. The Ising spin glass has been well realized in a mixed Ising antiferromagnet. Most of the predicted spin glass behavior has been verified by the experiments. Antiferromagnets will surely continue to play a crucial role in future investigations of systems with quenched disorder.

Acknowledgements

For those experiments described here in which I participated, I would like to thank Vincent Jaccarino for use of the high quality crystals and for very helpful discussions. I would also like to thank Allan King in particular for his advice and collaboration in many of the early random-field and random-exchange experiments. I have enjoyed many collaborations on the experiments mentioned in this review including those with R. Cowley, H. Dow, R. Erwin, B. Farago, I. Ferreira, S.-J. Han, W. Kleemann, C. Lartigue, D. Lederman, R. Lui, F. Mezei, F. C. Montenegro, R. Nicklow, P. Pollak, C. Ramos, S. Al. Rezende, J. Wang and H. Yoshizawa. Among the many theorists who have contributed greatly to my understanding of these topics are J. Cardy, U. Nowak, Y. Sliapir and A. P. Young. This work is supported by Department of Energy grant No. DE-FG03-87ER45324.

References

1. D. P. Belanger, *Phase Transitions* **11**, 53 (1988).
2. D. P. Belanger and A. P. Young, *J. Magn. Magn. Mater.* **100**, 272 (1991).
3. R. A. Cowley, *Physica B* **180-181**, 21 (1992).
4. T. Nattermann, *Ferroelectrics* **104**, 171 (1990).
5. Y. Sliapir in *Recent Progress in Random Magnets*, ed. by D. H. Ryan (World Scientific, Singapore, 1992).
6. T. Nattermann and J. Villain, *Phase Trans.* **11**, 817 (1988).
7. V. Jaccarino and A. R. King, *New Trends in Magnetism*, ed. by A. D. Coutinho-Filho and S. M. Rezende, (World Scientific, Singapore, 1989).
8. K. H. Fischer and J. A. Hertz, *Spin Glasses* (Cambridge University Press, Cambridge, 1991).
9. K. Binder and A. P. Young, *Rev. Mod. Phys.* **58**, 801 (1986).
10. D. P. Belanger, P. Nordblad, A. R. King, V. Jaccarino, L. Lundgren and O. Beckman, *J. Magn. Magn. Mater.* **31-34**, 1005 (1983).
11. D. P. Belanger and H. Yoshizawa, *Pliys. Rev. B* **35**, 4823 (1987).
12. G. K. Wertheim and D. N. E. Buchanan, *Phys. Rev.* **161**, 478 (1967).
13. D. P. Belanger, B. Farago, V. Jaccarino, A. R. King, C. Lartigue and F. Mezei, *J. de Phys.* **49**, CS-1229 (1988).
14. J. C. Le Guillou and J. Zinn-Justin, *Phys. Rev. Lett.* **39**, 95 (1977).
15. E. Brezin, J. C. Le Guillou and J. Zinn-Justin, *Phys. Lett.* **47A**, 285 (1974).
16. R. E. Fisher and R. J. Burford, *Pliys. Rev.* **156**, 583 (1967).
17. H. B. Tarko and A. E. Fisher, *Phys. Rev. B* **11**, 1217 (1975).

18. P. C. Hohenberg and B. I. Halperin, *Rev. Mod. Phys.* **49**, 435 (1977).
19. M. T. Hutchings, B. D. Rainford and H. J. Guggenheim, *J. Phys. C* **3**, 307 (1970).
20. P. Nordblad, D. P. Belanger, A. R. King, V. Jaccarino and H. Ikeda, *Pliys. Rev. B* **38**, 278 (1983).
21. L. Onsager, *Phys. Rev.* **65**, 117 (1914).
22. R. A. Cowley, M. Hagen and D. P. Belanger, *J. Phys. C* **17**, 3763 (1984).
23. C. A. Tracy and B. McCoy, *Phys. Rev. B* **12**, 368 (1975).
24. A. D. Bruce, *J. Phys. C* **14**, 193 (1981).
25. M. Hagen and D. McK. Paul, *J. Phys. C* **17**, 5605 (1984).
26. D. P. Belanger, S.-J. Han, V. Jaccarino, A. R. King, D. Lederman, R. Lui, R. R. Nicklow, C. A. Ramos, and J. Wang, unpublished.
27. Many of the highest quality crystals used in the $d = 3$ experiments have been grown at the UCSB Material Preparation Laboratory by N. Nighman.
28. A. R. McGurn and R. A. Tahir-Kheli, *Phys. Rev. B* **18**, 503 (1978).
29. C. B. de Araújo, *Phys. Rev. B* **22**, 266 (1980), and references therein.
30. H. Ikeda, *J. Phys. Soc. Japan* **50**, 3215 (1981).
31. A. B. Harris, *J. Phys. C* **7**, 1671 (1974).
32. S. Fisman and A. Aharony, *J. Phys. C* **12**, L729 (1979).
33. P. H. Barrett, *Pliys. Rev. B* **34**, 3513 (1986).
34. I. B. Ferreira, J. L. Cardy, A. R. King and V. Jaccarino, *J. Appl. Phys.* **69**, 5075 (1991).
35. R. J. Birgeneau, R. A. Cowley, G. Sliirane, H. Yoshizawa, D. P. Belanger, A. R. King and V. Jaccarino *Pliys. Rev. B* **27**, 6747 (1983).
36. J. Wang and D. P. Belanger, unpublished.
37. K. E. Dow and D. P. Belanger, *Phys. Rev. B* **39**, 4418 (1989).
38. K. E. Newman and E. K. Riedel, *Phys. Rev. B* **25**, 264 (1982).
39. G. Jug, *Pliys. Rev. B* **27**, 609 (1983).
40. S. A. Newlove, *J. Phys. C* **16**, L423 (1983).
41. N. A. Shpot, *Sov. Phys. JETP* **71**, 989 (1990).
42. D. P. Belanger, A. R. King and V. Jaccarino, *Pliys. Rev. B* **34**, 452 (1986).
43. R. A. Pelcovits and A. Aharony, *Phys. Rev. B* **31**, 350 (1985).
44. N. Rosov, A. Kleinhammes, P. Lidbjork, C. Hoehenemser, and A. Eibschütz, *Phys. Rev. B* **37**, 3265 (1988).
45. V. S. Dotsenko and V. S. Dotsenko, *J. Phys. C* **15**, 495 (1983); *J. Phys. C* **15**, L557 (1983); *Adv. Phys.* **32**, 129 (1983).
46. R. Sliankar, *Pliys. Rev. Lett.* **58**, 2466 (1987).
47. I. O. Mayer, *J. Phys. A* **22**, 2815 (1989); I. O. Mayer, 4. I. Sokolov and B. N. Shalaye, *Ferroelectrics* **95**, 93 (1989).
48. I. B. Ferreira, A. R. King, V. Jaccarino, J. L. Cardy and H. J. Guggenheim, *Phys. Rev. B* **28**, 5192 (1983).
49. M. Hagen, R. A. Cowley, R. M. Nicklow and H. Ikeda, *Phys. Rev. B* **36**, 401 (1987).
50. Y. Imry and S.-K. Ma, *Pliys. Rev. Lett.* **35**, 1399 (1975).
51. J. Cardy, *Pliys. Rev. B* **29**, 505 (1984).
52. D. P. Belanger, A. R. King, V. Jaccarino and J. L. Cardy, *Phys. Rev. B* **28**, 2522 (1983).
53. J. Z. Imbrie, *Pliys. Rev. Lett.* **53**, 1747 (1984).
54. J. Brimont and A. Kupiainen, *Pliys. Rev. Lett.* **59**, 1829 (1987).
55. M. Mezard and A. P. Young, *Phys. Rev. Lett.* **18**, 653 (1992).
56. D. P. Belanger, A. R. King and V. Jaccarino, *Phys. Rev. B* **31**, 4538 (1985).
57. A. Aharony, Y. Imry, and S. K. Ma, *Pliys. Rev. Lett.* **37**, 1364 (1976).
58. A. P. Young, *J. Phys. A* **10**, L257 (1977).
59. G. Parisi and N. Sourlas, *Phys. Rev. Lett.* **43**, 744 (1979).
60. C. A. Ramos, A. R. King, V. Jaccarino and S. M. Rezende, *J. de Phys.* **49**, C8-1241 (1988).
61. A. Aharony, *Europhys. Lett.* **1**, 617 (1986).
62. D. P. Belanger, A. R. King, V. Jaccarino and R. M. Nicklow, *Pliys. Rev. Lett.* **59**, 930 (1987).
63. I. B. Ferreira, A. R. King and V. Jaccarino, *Phys. Rev. B* **43**, 10797 (1991).
64. D. P. Belanger, A. R. King, I. B. Ferreira and V. Jaccarino, *Pliys. Rev. B* **37**, 226 (1988).
65. A. E. Nash, A. R. King and V. Jaccarino, *Pliys. Rev. B* **43**, 1272 (1991).
66. A. R. King, J. A. Mydosh and V. Jaccarino, *Phys. Rev. Lett.* **56**, 2525 (1986).
67. J. Villain, *J. Phys. Lett.* **43**, L551 (1982); *J. de Phys.* **46**, 1843 (1985).
68. D. S. Fisher, *Phys. Rev. Lett.* **56**, 416 (1986).
69. J. P. Hill, T. R. Thurston, R. W. Erwin, M. J. Ramstad and R. J. Birgeneau, *Pliys. Rev. Lett.* **66**, 3281 (1991). In this work on a weakly anisotropic system, the authors claim to be the first to observe the RFIM transition, disregarding all previous work on this subject in which the critical behavior has been studied. At low enough field and large enough magnetic concentration the line shapes will of course be resolution limited as observed in this work. The problem is in interpretations relying solely on the width of the diffuse scattering peaks for which a precise theoretical form is unknown. The same method has been used to incorrectly deduce that there is no RFIM transition⁹⁷, and that the transition is first order⁹⁸, both in the same system used above.
70. P. Pollak, W. Kleemann and D. P. Belanger, *Phys. Rev. B* **38**, 4773 (1988).
71. Y. Shapiro, *Phys. Rev. B* **35**, 62 (1987); *Phys. Rev. Lett.* **54**, 154 (1985); *J. Phys. C* **17**, L809

- (1984).
72. D. P. Belanger and H. Yosliizawa, unpublished.
 73. D. P. Belanger, A. R. Kings, and V. Jaccarino, unpublished.
 74. A. R. King, V. Jaccarino, A. Motokawa, K. Sugiyama and M. Date, *J. Appl. Phys.* **57**, 3297 (1985).
 75. D. P. Belanger, A. R. King and V. Jaccarino, *Phys. Rev. Lett.* **54**, 577 (1985).
 76. H. Yosliizawa, R. A. Cowley, G. Sliirane, R. J. Birgeneau, H. J. Guggenheim and H. Ikeda, *Phys. Rev. Lett.* **48**, 438 (1982).
 77. D. P. Belanger, A. R. King and V. Jaccarino, *Sol. St. Comm.* **54**, 79 (1985).
 78. W. Kleemann, A. R. King and V. Jaccarino, *Phys. Rev. B* **34**, 479 (1986).
 79. U. Nowak and K. D. Usadel, *Phys. Rev. B* **44**, 7426 (1991).
 80. U. Nowak and K. D. Usadel, *Physica B* **165**, 211 (1990).
 81. U. Nowak and K. D. Usadel, *Phys. Rev. B* **46**, 8329 (1992).
 82. S.-J. Han and D. P. Belanger, *Phys. Rev. B* **46**, 2926 (1992).
 83. It has recently been pointed out by T. Nattermann in a private communication that power law behavior is also consistent with the original N-V picture of microscopic domain wall rearrangements if the power law dependence of AE on the length scale L is replaced by a logarithmic one. This transforms the logarithmic time dependence of the remanent magnetization given in the original N-V theory into a power law dependence.
 84. U. Nowak and K. D. Usadel, *Phys. Rev. B* **43**, 851 (1991).
 85. S.-J. Han, D. P. Belanger, W. Kleemann and U. Nowak, *Phys. Rev. B* **45**, 9728 (1992).
 86. R. Lederman, J. V. Selinger, R. Bruinsma, J. Hammann and R. Orbach, *Phys. Rev. Lett.* **68**, 2086 (1992); M. Lederinan, J. V. Selinger, R. Bruinsma, R. Orbach and J. Hammann, unpublished.
 87. R. Bruinsma and G. Aeppli, *Phys. Rev. Lett.* **52**, 1547 (1984).
 88. R. A. Cowley, G. Sliirane, R. J. Birgeneau, E. C. Svensson and H. J. Guggenheim, *Phys. Rev. B* **22**, 4412 (1980).
 89. F. C. Montenegro, S. R. Rezende and M. D. Coutinho-Filho, *J. Appl. Phys.* **63**, 3755 (1988); S. A. Rezende, F. C. Montenegro, A. D. Coutinho-Filho, C. C. Becerra and A. Paduan-Filho, *J. de Phys.* **49**, C8-1267 (1989); F. C. Montenegro, R. D. Coutinho-Filho and S. M. Rezende, *Europhys. Lett.* **8**, 382 (1989).
 90. S. A. Rezende, F. C. Montenegro, U. A. Leitão and R. D. Coutinho-Filho *New Trends in Magnetism*, ed. by A. D. Coutinho-Filho and S. M. Rezende, (World Scientific, Singapore, 1980); and F. C. Montenegro, U. A. Leitão, M. D. Coutinho-Filho and S. M. Rezende, *J. Appl. Phys.* **67**, 5243 (1990).
 91. J. R. L. de Almeida and D. J. Thouless, *J. Phys. A* **11**, 983 (1978).
 92. F. C. Montenegro, A. R. King, V. Jaccarino, S.-J. Han and D. P. Belanger, *Phys. Rev. B* **44**, 2155 (1991); D. P. Belanger, Wm. E. Murray, Jr., F. C. Montenegro, A. R. King, V. Jaccarino and R. W. Erwin, *Phys. Rev. B* **44**, 2161 (1991).
 93. C. L. Henley, *Phys. Rev. Lett.* **54**, 2030 (1985).
 94. H. Yosliizawa, S. Mitsuda, H. Aruga and A. Ito, *Phys. Rev. Lett.* **59**, 2364 (1987); *J. Phys. Soc. Japan* **58**, 1416 (1989).
 95. H. Yosliizawa, H. Mori, S. Mitsuda, H. Aruga, H. Kawano, S. Ebii and A. Ito, *Physica B* **180-181**, 209 (1992).
 96. H. A. Katori, T. Goto, S. Ebii and A. Ito, *J. Mag. Mag. Mat.* **104-107**, 1639 (1992); H. Aruga, A. Ito, H. Wakabayashi and T. Goto, *Physica B* **155**, 311 (1989); H. Aruga, A. Ito, H. Wakabayashi, and T. Goto; H. Yoshizawa, H. Mori, S. Mitsuda, H. Aruga Katori, and A. Ito, unpublished; H. Aruga, A. Ito, H. Wakabayashi and T. Goto, *J. Phys. Soc. Japan* **57**, 2636 (1988).
 97. R. J. Birgeneau, Y. Shapira, G. Shirane, R. h. Cowley and H. Yoshizawa, *Physica* **13713**, 83 (1986).
 98. R. J. Birgeneau, R. A. Cowley, G. Sliirane and H. Yosliizawa, *Phys. Rev. Lett.* **54**, 2147 (1985).